Volume 1 | Number 1 | Jan 2013 | Pages 1–100

Nanoscale

www.rsc.org/nanoscale

ROYAL SOCIETY OF CHEMISTRY

www.rsc.org/nanoscale

Nanoscale

FEATURE ARTICLE

Graphene supported non-precious metal-macrocycle catalysts for oxygen reduction reaction in fuel cells

Hyun-Jung Choi,[a]† Nanjundan Ashok Kumar,[a]† and Jong-Beom Baek[a*]

Fuel cells are promising alternative energy devices owing to its high efficiency and eco-friendliness. While platinum is generally used as a catalyst for the oxygen reduction reaction (ORR) in a typical fuel cell, limited reserves and prohibitively high costs limits its future use. The developments of non-precious and durable metal catalysts are being constantly conceived. Graphene has been widely used as substrate for metal catalysts due to its unique properties, thus improving stability and ORR activities. In this feature, we present an overview on the electrochemical characteristics of graphene supported non-precious metal containing macrocycle catalysts that include metal porphyrin and phthalocyanine derivatives. Suggested research and future development directions are discussed.

Introduction

The alarming increase of environmental pollution and ever increasing energy consumption has turned research attention towards clean and energy efficient alternative systems. Lithium ion batteries (LIBs), supercapacitors and fuel cells show promise to meet the colossal energy demand. Fuel cells are devices that directly convert chemical energy from a fuel into electricity by an electrochemical reaction,[1-3] and are in par with supercapacitors and LIBs. With near zero emission of pollutants, high power density and high energy-conversion, fuel cell technology is swiftly shifting from basic research towards commercial development.[4,5] Typical fuel cells consist of an anode, cathode and a membrane. At the cathode, electrochemical fuel oxygen reduction reaction (ORR) and oxygen evolution reaction (OER) take place, whereas hydrogen oxidation reaction (HOR) and hydrogen evolution reaction (HER) takes place at the anode.[6] The challenging and current bottleneck lies in the sluggish ORR kinetics on the cathode that significantly limits the efficiency and performance of the fuel cell device. Because platinum-based (Pt) electrocatalysts have been traditionally used to catalyze the ORR, a fuel cell stack alone accounts up to 50% of the cost of the whole system.[7]

Although Pt-based composites are most efficient cathode catalysts, they still suffer from serious drawbacks that include crossover poisoning, low stability, especially in acidic media thus leading to declined activity or performance loss. Most important of all, limited reserves and prohibitively high cost hinder the wide spread commercialisation of fuel cells in general. Therefore, exploring new electrocatalysts with enhanced ORR activities and stabilities for the replacement of this costly noble metal with non-precious alternatives is highly warranted and is of paramount importance to commercialise fuel cells as well as for other renewable energy applications. In the intensifying search for durable and efficient materials, researchers have tried to reduce the amount of Pt used by lowering platinum usage,[8-10] use of non-precious metal catalyst[11,12] that are abundant in nature and also metal free catalyst for ORR have been actively explored.[13-18] Obviously, the latter two hold astounding importance in realising cheap fuel cell technology. Up to day, various types of non-precious ORR catalysts have been investigated and detailed in recent accounts, which include, graphene and graphene based derivatives,[19] doped-carbon materials,[20] metal containing carbon nitrides supported on graphene,[21] as well as transition metal chalcogenides.[22]

Apart from the above-mentioned materials, the use of transition metal containing N_4 chelate macrocycle complexes to catalyze ORR have attracted wide attention ever since Raymond Jasinski pioneered and reported the activity of cobalt pthalocyanines as a fuel cell cathode catalyst in 1964.[23] Since then, many metal containing N_4 chelate macrocycle complexes such as phthalocyanines and porphyrins, have been widely investigated for ORR activity in fuel cells. In addition, the incorporation of such a metal containing macrocycle with graphene or other carbon material for enhanced ORR activity has been recognized in the recent past. Especially, graphene, which is a two-dimensional sheet composed of sp^2-hybridised

conjugated carbon atoms remains a material of choice[24] because graphene acts as a new class of support material for metal catalysts owing to its excellent electrical conductivity,[24] large surface area,[25] chemical[26] and mechanical stability,[27] eventually increasing the stability and improving the electrocatalytic activities in ORR reactions. Albeit in its nascent stage, considerable amount of work has been done recently and herein, we review important advances involving such a metal containing macrocycle with carbon-based composite structure in ORR enhancement. We highlight important results, especially, with graphene supported composites and discuss the role of other carbon structures and their influences in catalyzing ORR. Future research strategies are also discussed in brief.

Metal macrocycle/graphene composites in ORR

Non-precious metal macrocycles, such as porphyrin (P) and phthalocyanines (Pc), have been deemed to be choice materials, because they have unique properties and show promising electrocatalytic activity that could be useful in various field including sensing,[28] optoelectronics,[29-33] capacitors,[34] and fuel cells.[35,36] In particular, transition metal N_4-macrocycles such as metal-P and metal-Pc, are very interesting materials to overcome the sluggish ORR kinetics in both alkaline and acid medium for fuel cells.[37-42] The catalytic activities of these kinds of electrocatalysts depend mainly on the core metal, the precursor, the supporting substrate, and the heat treatment temperature. In principle, C, N, and Fe (or Co) are necessary to obtain active sites. Here, we mainly discuss the influence of the core metal, Co and Fe precursors containing nitrogen, P and Pc on the elctrocatalytic activities towards ORR. A multidenate ligand is called chelating ligand, if on co-ordination forms a cyclic or closed ring. This complex is called chelate, which is more stable than a non-cyclic or open complex compound, or the macrocyclic effect. Prominent among them are metal complexes with macrocyclic ligands that contain four nitrogen donors (metal-N_4 chelates), adsorbed on carbon supported and heat treated of resulting materials in an inert atmospheres.[43] The stoichiometric value of 4.0 is an ideal metal-N_4 macrocyclic structure, while the non-stoichiometric metal content indicated that some of the nitrogen could not integrate with metal to form catalytic active sites.

Metal porphyrin/graphene composites in ORR

Metalloporphyrin catalysts have been extensively explored as a potential replacement for Pt in the catalysis of the ORRs. Loh and co-workers synthesised a hybrid metal organic framework (MOF) by addition of pyridinium dye-functionalized rGO (G-dye) sheets to iron-porphyrin frameworks.[44] The chemical structures of the various subunits in the assembled MOF are illustrated in Fig. 1. The MOF is created by linking the porphyrin, namely, 5,10,15,20-tetrakis(4-carboxyl)-21H,23H-porphyrin (TCPP) and $FeCl_3$ (Fe−P)$_n$ MOF to yield (G-dye-FeP)$_n$ MOF. Here, the G-dye represents rGO sheets that are

functionalized with π-electron donor-acceptor dye, which terminates in pyridinium moieties (electron-withdrawing systems by stabilizing the electron-rich phenylethyl group, and prevents aggregation). The electroactive surface area of 50 wt.% G-dye mixed with (Fe-P)$_n$ MOF clearly shows that the incorporation of G-dye increases the electroactive surface area of the electrode and enhances charge transfer kinetics. The cathodic current peaks of -0.23 V within the potentials of -0.8 V to 0.3 V in O_2 saturated 0.1 M KOH, was obtained for the (G-dye 50 wt.%-FeP)$_n$ MOF, which is higher than that of exfoliated graphene (-0.44 V) and GO (-0.35 V). The electron transfer number n of (Fe-P)$_n$ MOF and GO for ORR was calculated to be between 2 to 4 which critically depended on the over potential, whereas the electron transfer number at the (G-dye 50 wt.%-FeP)$_n$ MOF electrode was always ~4, and independent of the potential tested. Synergistic effects of framework porosity, larger bond polarity due to the presence of nitrogen ligand in the G-dye and the catalytically active iron−porphyrin in the structure of the hybrid MOF were attributed to the improvements in the catalytic activity.
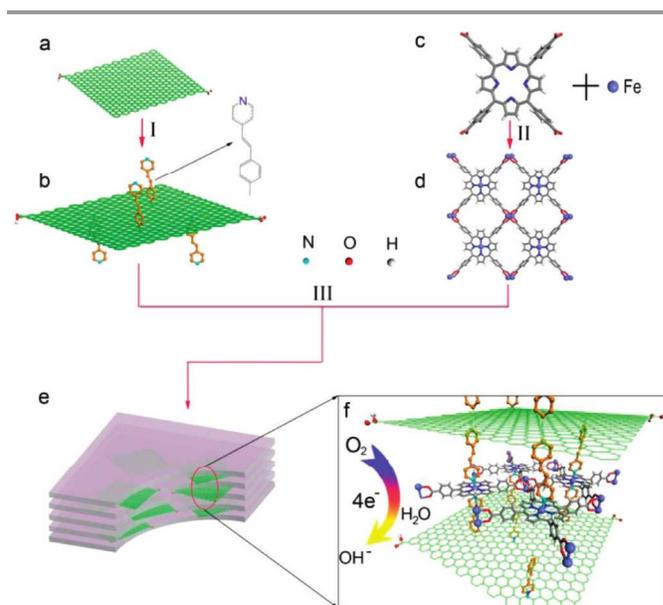

Fig. 1. Schematic of the Chemical Structures of (a) Reduced GO (r-GO), (b) G-dye, (c) TCPP, (d) (Fe−P)$_n$ MOF, (e) (G-dye-FeP)$_n$ MOF, and (f) Magnified View of Layers Inside the Framework of (G-dye-FeP)$_n$. (Reproduced from ref. 44 with permission. Copyright 2012, American Chemical Society)

Similarly, Tang *et al*. studied the influence of cobalt porphyrin multilayers decorated on rGO sheet for ORR.[45] Using a layer by layer assembly technique, Co^{2+}-rGO with 5,10,15,20-tetrakis(4-hydroxyphenyl) porphyrin (THPP) (rGO/Co^{2+}-THPP)$_n$; [n is cycle number of one composite layer of Co^{2+} and THPP] were synthesised (Fig. 2a). The LBL assembly method can be efficiently control the structure and thickness of the Co^{2+}-THPP layers on to the rGO substrate.[46] The ORR activity increased until the 5 layers of rGO/Co^{2+}-

THPP$_n$ composites and over 5 layers, it shows similar ORR performance. This result indicated that the optimised number of Co^{2+}-THPP layers improves electrocatalytic activity, while, over 5 layers of Co^{2+}-THPP layers interrupt diffusion of both O$_2$ and electrolyte towards the inner Co^{2+}-THPP layers. The limiting current density of rGO/Co^{2+}-THPP$_7$ at -1.0 V was up to about -4.0 mA cm^{-2} that was comparable to C/Pt (Fig. 2b) and higher than other rGO based materials. It was shown that the composite had better stability after 40,000s (c.a. 80%) and better tolerance of methanol crossover compared with C/Pt (Fig. 2c).

Electrochemical reduction of cobalt[5,15-(p-aminophenyl)10,20(pentafluorophenyl)-porphyrin] functionalized GO (ERGO-CoAPFP) was also carried out.[45,47] The half wave potential ($E_{1/2}$) of O$_2$ reduction for the ERGO-CoAPFP (-0.19 V) was positive than that of GO supported material. This result demonstrated that cobalt plays a significant role in improving the ORR catalytic activity with enhanced electron transfer reaction than that of GO. The O$_2$ reduction onset potential of ERGO-CoAPFP was about -0.054V with high ORR current. In addition, the composite follows a favourable 4-electron transfer pathway (n>3.8) and much lower H$_2$O$_2$ production than that of a GO based material was noticed. In addition, ERGO-CoAPFP also exhibited much better tolerance to methanol and ethanol than that of commercial Pt/C with long term stability compared to Pt/C after 2.5 hours.
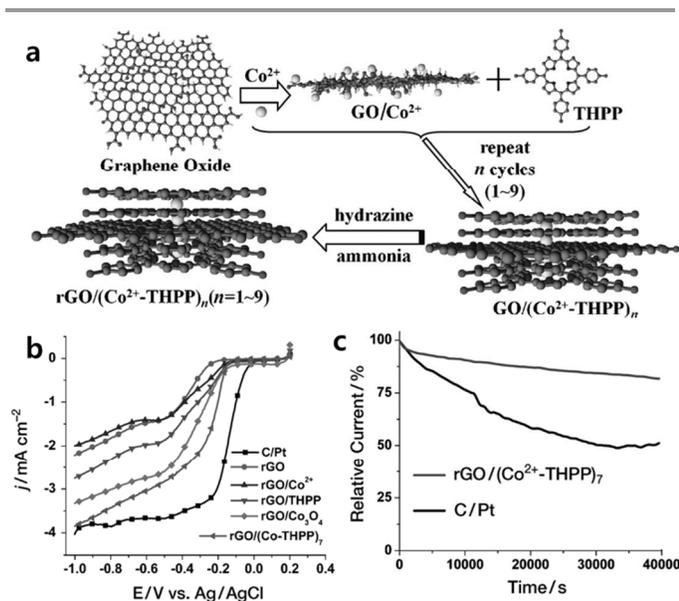
Very recently, Jaing et $al.$ developed a series of non-noble-metal catalysts for oxygen reduction reaction (ORR), based on metal 5,10,15,20- tetrakis(4-hydroxyphenyl)porphyrin (M-THPP; M:Fe^{3+}, Co^{2+}, Ni^{2+}, Mn^{2+}) grown on poly(sodium-p-styrenesulfonate) functionalized rGO (M-THPP/PSS-rGO) by using an in $situ$ solvothermal synthesis method.[48] This method can be regarded as effective and commercially viable method because of many merits such as the possibility to control the morphology, inexpensive raw materials, and low growth temperature. The ORR catalytic activity of M-THPP/PSS-rGO based on half wave potential were found to be in the order of: CoTHPP/PSS-rGO (-0.22 V $vs.$ SCE) > MnTHPP/PSS-rGO (-0.32 V $vs.$ SCE) > FeTHPP/PSS-rGO (-0.38 V $vs.$ SCE) > NiTHPP/PSS-rGO (-0.40 V $vs.$ SCE) (Fig. 3a). Electron transfer number of M-THPP/PSS-rGO, ranked in descending order are as follows this order: CoTHPP/PSS-rGO (3.79-3.83) > FeTHPP/PSS-rGO (3.69-3.80) > MnTHPP/PSS-rGO (3.19-3.72) > NiTHPP/PSS-rGO (2.65-2.82) (Fig. 3b). The CoTHPP/PSS-rGO composites show the lowest production of HO$_2^-$ (8.60-10.70%) of the M-THPP/PSS-rGO (Fig. 3c). These results indicate that CoTHPP/PSS-rGO is best suitable catalyst among other metal based porphyrins used and also throw light that the electrocatalytic activities of these M-THPP/PSS-rGO can be affected by the nature of the central metal.
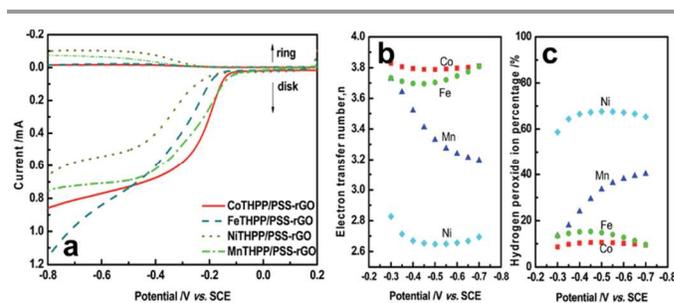

Fig. 3. (a) RRDE tests for the ORR on M-THPP/PSS-rGO in O$_2$-saturated 0.1M NaOH at a rotation speed of 1600 rpm. (b) Electron transfer number and (c) hydrogen peroxide ion percentage of CoTHPP/PSS-rGO, FeTHPP/PSS-rGO, MnTHPP/PSS-rGO and NiTHPP/PSS-rGO. (Reproduced from ref. 48 with permission. Copyright 2014, Royal Society of Chemistry)

Fig. 2. (a) Preparation procedure of rGO/(Co^{2+}–THPP)$_n$. (b) LSV on RDE of rGO, rGO/Co^{2+}, rGO/THPP, rGO/Co$_3$O$_4$, rGO/(Co^{2+}–THPP)$_7$, and C/Pt in O$_2$-saturated 0.1M KOH solution with a sweep rate of 10 mV/s at a RDE rotation rate of 1600 rpm, and (c) normalized I–t chronoamperometric responses of rGO/(Co^{2+}–THPP)$_7$ and C/Pt at -0.25 V in O$_2$ saturated 0.1 M KOH solution at a rotating rate of 1000 rpm. . (Reproduced from ref. 45 with permission. Copyright 2013, John Wiley & Sons)

Generally, metal-porphyrin-graphene composites shows excellent electrochemical activities for ORR with ~4 electron transferred behaviour and they exhibit better stability >80% than commercial Pt/C with outstanding alcohol crossover tolerance.

Metal phthalocyanine/graphene composites in ORR

Very recently, Yin et $al.$ reported the formation of a 3D iron nitride/nitrogen doped-graphene aerogel hybrid, in which iron phthalocyanine was uniformly dispersed and anchored on graphene surface with the assist of π–π stacking and oxygen-containing functional groups and studied their ORR activity. By using FePc as Fe precursors, a simple hydrothermal process could in situ grow Fe$_x$N nanoparticles on to the graphene layer

in NH_3 atmosphere,[49] (Fig. 4a). While acting as a precursor of Fe and Nitrogen, FePc not only prevents the restacking between GO layer, a porous morphology with high surface area could also be obtained.[50] In addition, FePc do not ionize H_2O and the π-π interactions can make stable suspension with GO without the use of any stabilizer.[49] The ORR activity of the synthesised 3D nitrogen doped (NG) graphene aerogel supported Fe_xN nanoparticles (Fe_xN/NGA) were then estimated by CV. The onset potential of Fe_xN/NGA appeared at 0.01 V vs. Ag/AgCl, which was slightly positive than that of commercial Pt/C (-0.12 V) (Fig. 4b). The catalytic activities obtained by CV were confirmed with RDE measurements (Fig. 4c). In addition, Fe_xN/NGA hybrid exhibited much lower Tafel slope (52 mV dec^{-1}) than Pt/C (68 mV dec^{-1}), and showed similar Nernstian Tefel slope (59 mV dec^{-1}) at low over potentials. This slope implied that the rate determining step of ORR was caused by the breaking of O-O bonds when two electrons transferred from active sites to adsorbed O_2 molecules and Fe (III) in Fe-N-C structure provided the sites for O_2 adsorption.[51] Moreover, from the electrochemical impedance spectroscopy measurement, it was shown that Fe_xN/NGA to have low electron transfer resistance with 10.5 Ω, small charge transfer resistance and mass transfer resistance. The Fe_xN/NGA hybrid does not affect methanol oxidation and were very stable for 20,000s at constant voltage of -0.4 V. The results indicate that the Fe_xN/NGA has comparable electrocatalytic activity for ORR than Pt/C at the same catalyst loading, while its stability and resistance to methanol crossover were found to be superior.
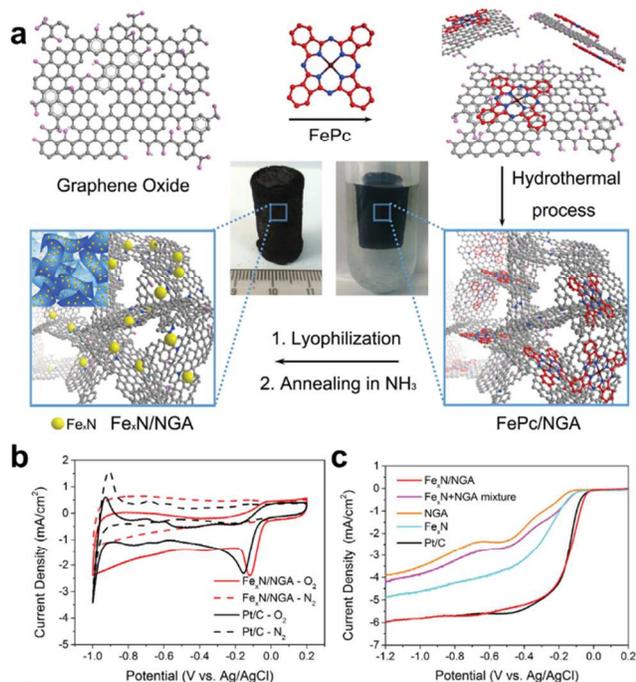
.

Fig. 4. (a) Scheme of the synthesis procedure of Fe_2N/NGA. (b) CV curves of Fe_xN/NGA hybrid and commercial Pt/C in O_2-saturated (solid line) or N_2–saturated (dash line) 0.1 M KOH. (c) RDE voltammograms of Fe_xN/NGA hybrid,

Fe_xN +NGA mixture, NGA, free Fe_xN and Pt/C in O_2-saturated 0.1 M KOH at a sweep rate of 10 mV s^{-1} at 1600 rpm. (Reproduced from ref. 49 with permission. Copyright 2014, John Wiley & Sons)

A similar strategy was also reported where iron phthalocyanine (FePc) and nitrogen doped graphene (NG) composite (FePc/NG), were synthesized by a solution process in the presence of GO and ammonia.[52] ORR activities of FePc/NG, were measured by CV and RDE. With a peak current at -0.14 V vs. Ag/AgCl, the CV showed a positively shifted (-0.01 V) onset potential than that of pristine FePc (-0.06 V) and NG (-0.08 V). Due to the improved electrical conductivity, the composites showed enhanced ORR activity compared to that of commercially available Pt/C. In addition, tolerance to methanol crossover in a direct methanol fuel cell (DMFC) was also demonstrated. In the case of FePc/NG, no significant change with and without 1M methanol, while Pt/C clearly showed an oxidation peak at -0.25 V after addition of methanol. This phenomena indicates that FePc/NG is very suitable for DMFCs with good methanol crossover tolerance.[35]

Stability and tolerance to alcohol crossover, fuel poisoning effect and long-term stability are also important issues in fuel cells. Therefore, iron tetrasulfophthalocyanine functionalized graphene nanosheets (GNs-FeTSPc) synthesized by noncovalent functionalization between GNs with FeTSPc by π-π stacking interaction through ultrasonication were tested for ORR activity (Fig. 5a).[39]
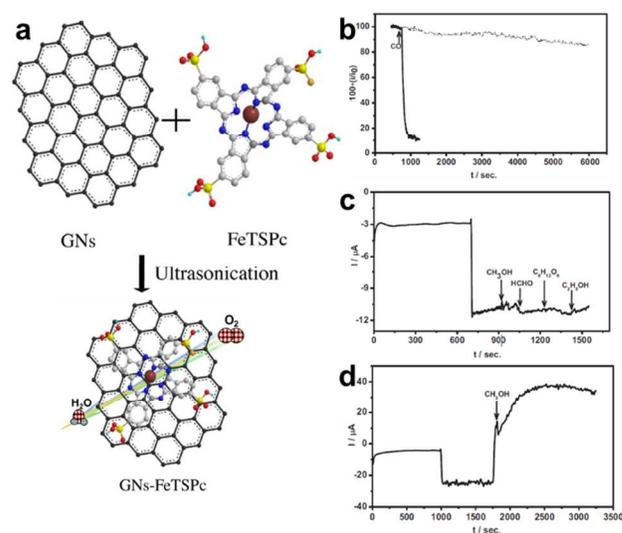

Fig. 5. (a) Illustration of noncovalently functionalized GNs with FeTSPc via a π-π stacking interaction. (b) CO-poisoning effect on the i-t chronoamperometric response at -0.3 V for Pt-C/GC (solid) and GNs-FeTSPc/GC (short dot). (c) i-t chronoamperometric response obtained at GNs-FeTSPc/GC electrode at -0.3 V in 0.1 M KOH. Then 3.0 M methanol, 1.0 M formaldehyde, 1.0 M glucose and 1.0 Methanol were added, respectively. (d) i-t chronoamperometric response obtained at the Pt-C/GC electrode with 3.0 M methanol. (Reproduced from ref. 39 with permission. Copyright 2014, Elsevier)

CO poisoning and crossover data of GNs-FeTSPc and Pt-C in Fig. 5b-d showed that GNs-FeTSPc had good tolerance from

CO poisoning effects, while the Pt-C was affected by CO injection. The carbonyl intermediates can strongly absorb onto the surface of the Pt-C, otherwise in case of FeTSPc, irons were located in centre of molecules which was protected by intensive planar heteroaromatic π conjugation systems, which were less affected by CO poisoning.[53] Moreover, fuel crossover occurred from the anode to the cathode. Four kinds of fuels including 3 M Methanol, 1 M formaldehyde, 1 M glucose and 1M ethanol were chosen to check the fuel crossover effects (Figs. 5c&d). The FeTSPc shows very good tolerance among all of four fuels, while the Pt-C shows rapidly increased methanol oxidation current due to methanol crossover. The authors concluded that GNs-FeTSPc composites can be used as an electrcatalyst for ORR in methanol, formaldehyde, glucose and ethanol fuel cells.

In another instance, iron phthalocyanine (FePc)/GO (g-FePc) synthesized through π-π interaction between FePc and GO.[54] Graphene, prevented agglomeration of the molecules during electrochemical test, and was homogeneously attached on to the surface of GO. The g-FePc shows a cathodic ORR peak at 0.9 V in presence of O_2 by CV measurement, which was more positive than Pt/C (0.85 V). The electron transfer number calculated by K-L plots was found to be 3.96~4.00 at 0.15~0.35 V. In addition, the HO_2^- of g-FePc produced < 3%. With long-term stability at about 84.0% and good tolerance from methanol crossover and CO poisoning and a 4-electron pathway these hybrids were rendered suitable for such fuel cell applications.

Cobalt(II) tetranitrophthalocyanine (CoTNPc) incorporated with poly(sodium-p-styrenesulfonate) functionalized graphene (PGr) (CoTNPc/PGr) composites were prepared by an *in-situ* solvothermal synthesis method.[55] CV measurement, indicate a cathodic peak potential of PGr and CoTNPc at *c.a.* -0.35 and c.a -0.39 V *vs.* SCE, respectively. On the other hand, the peak potential for CoTNPc/PGr was founded to be -0.22 V which is positively shifted compared to PGr and CoTNPc and much similar with Pt/C. LSV on RDE measurement were carried out to further investigate the ORR activity. An onset potential at *c.a.* -0.10 V vs SCE was found for CoTNPc/PGr. This material exhibits better ORR activity compared to that of PGr and CoTNPc and similar with PtC (-0.05 V) and follows a favorable 4 electron pathway. These hybrid materials show reasonable stability with retention of 69.9% after 24h, while Pt/C stability dramatic decreased to 13.3% after 24h. Undoubtedly, graphene supported phthalocyanine/non-precious metal catalysts shows good stability during long-term chronoampherometric experiments, and outstanding tolerance to fuels and CO poisoning. In majority of the case studies, the electrocatalytic activity follows a 4-electon pathway, with similar onset potential and better current density better or similar performance to commercially available Pt/C. Above studies indicate that such hybrids are vital to replace expensive and noble Pt based catalysts.

Catalytic role of other nanocarbon materials and their composite derivatives for ORR

In general, carbon based materials have widely been used as supporting substrate for non-precious metal catalysts owing to its advantageous chemical/thermal properties,[56,57] mechanical stability[27] large surface area,[25] and pore volumes. Carbon based materials, including carbon nanotube (CNT),[58-60] carbon black,[61-65] carbon nanosphere[66] and covalent organic polymer (COP),[67] aids the stability of the hybrid. In this section, we highlight the role of such carbon substrates other than graphene as support matrices for non-precious metal-macrocycle composites.

The formation of covalent network of porphyrins around MWNT surfaces by the adsorption of cobalt(II) meso-tetraethynylporphyrins on the nanotube sidewalls followed by the dimerization of the triple bonds *via* Hay-coupling was reported (Fig. 6).[58]
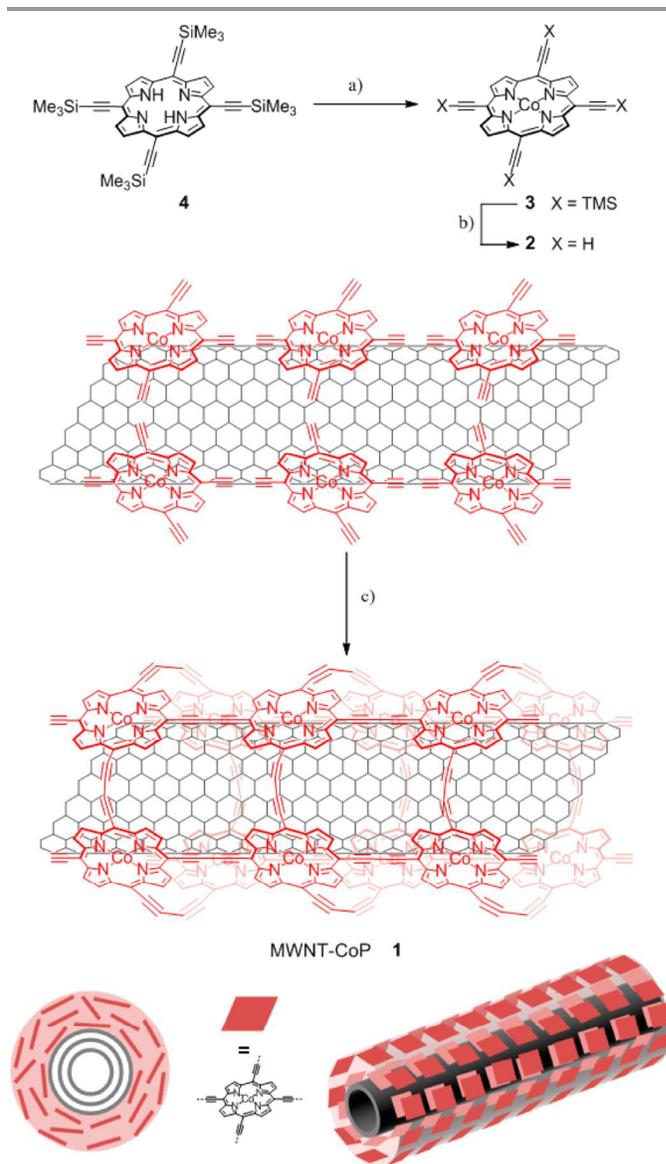

Fig. 6. Scheme of Synthesis of MWNT–CoP.[a]

Here, the CNT acts as a template for the formation of the polymeric layer. The hybrid material (MWNT-CoP) had pronounced stability resulting from the cooperative effect of the multiple π-stacking interactions between the porphyrins and the nanotube and by the covalent links between the porphyrins. The nanotube hybrids when tested as the supported catalyst for the oxygen reduction reaction (ORR) in a series of electrochemical measurements under acidic conditions, showed improved catalytic performances with an average value of transferred electrons that was close to 4.

A similar work reported by Guan and coworkers[59] studied the ORR activity of Iron(II) phthalocyanine coated on single-walled carbon nanotubes (FePc/SWCNTs) in alkaline medium. The over potential of FePc/SWCNTs (20 wt.% FePc) was almost the same with commercial Pt/C (20 wt.% Pt), while the current was higher. FePc/SWCNTs also exhibited excellent tolerance to the crossover effect, when methanol coexisted with oxygen in alkaline medium. The measured over potential values were -0.18 V for FePc, -0.30 V for SWCNTs, and about -0.16 V for FePc/SWCNTs in O$_2$ saturated 0.1 M NaOH solution. LSV shows that the onset potential for the FePc/SWCNTs started at about -0.02 V and was constant under different rotation speeds. The half-wave potential for the ORR was about -0.10 V for the FePc/SWCNTs. These two potentials were almost the same as those for the Pt/C. However, the ORR limiting currents for the FePc/SWCNTs were higher than those for the Pt/C under the same rotation rate. The transferred electron number per oxygen molecule on the FePc/SWCNTs involved in the ORR was 3.7~4.0 at the potential range of -0.40 ~ -0.70 V.

Similarly, Cobalt phthalocyanine (CoPc) assemblies were prepared using several kinds of MWNT templates by *in situ* solid synthesis in a muffle furnace.[60] The assemblies of CoPc/MWCNTs using acid functionalized MWNTs ranging from 10 to 30 nm in the outer diameter (OD) exhibited higher thermal stability. The obtained MWCNT-templated CoPc assemblies with coaxial nanotube structure exhibit higher catalytic activity. Depending on their assembled structures, they displayed different electrochemical characteristics. A novel g-C$_3$N$_4$-derived non-precious metal catalyst with high ORR activity and stability in acidic medium, was prepared by *in situ* polymerizing Fe-doped graphitic carbon nitride on carbon black (Fe−g-C$_3$N$_4$@C).[61] RDE/RRDE tests demonstrate that the pyrolyzed 10% Fe−N−C (750 °C) composite exhibits excellent ORR activity, almost four electron transfer processes, and better durability in comparison to Pt/C in acid electrolyte,

In another approach, Kim *et al.* were synthesized Fe-phthalocyanine based mesoporous carbon (FP-MCS) and phthalocyanine based mesoporous carbon (P-MCS) via solution plasma process in the benzene/dodecane.[66] From the CV data, cathodic peak and onset potential of P-MCS showed at -0.22 V and -0.09 V, respectively. In the case of FP-MCS, not only

cathodic peak and onset potential were slightly shifted to -0.17 V and -0.04 V, respectively, but also current density increased from -2.3 (P-MCS) to -3.5 mA cm^{-2} (FP-MCS), and the half wave potential was shifted from -0.18 V to -0.12 V when P-MCS was exchanged with FP-MCS. After the 20,000s, the current density loss of FP-MCS-3 was only 7%, implying excellent stability compared with P-MCS (17%). These results implied that Fe-N$_4$ site big improved the ORR activities leading to good stability.

In another interesting approach, 2D covalent organic polymer complexes (COP) with non-noble metals (M=Fe, Co, or Mn) prepared by Yamamoto polycondensation and were used as catalysts for ORR by Dai and co-workers.[67] Additional heat treatment could further carbonise into C-COP materials (C-COP-P-M) in order to form the regular metal/nitrogen distribution and good stability in acidic and alkaline medium (Fig. 7a). CV measured the electrocatalytic activities of samples. The peak potential and current density of all of the three C-COP-P-M shows more positive and higher current density than metal free 2D-COP (C-COP-P). Especially, peak potential of C-COP-P-Fe and C-COP-P-Co samples were at 0.77 V *vs.* RHE, (increased to 60%) compared to C-COP-P. Carbonization temperature was also tested to find the optimal temperature for ORR performances. It was found that the electrocatalytic activity was significantly improved at 950 °C. At temperature below 950 °C, carbonization would not lead to enough graphitization to establish high conductivity. On the other hand, when carbonization temperature over 950 °C, the conjugated structure of the C-COP-P framework were decomposed leading to lower conductivity. The linear sweep voltammogram shows that the onset potential of C-COP-P-Fe was similar to that of commercially available Pt/C (0.98 V *vs.* RHE) and the C-COP-P-Co showed a higher limiting current density than that of the Pt/C (Fig. 7b).
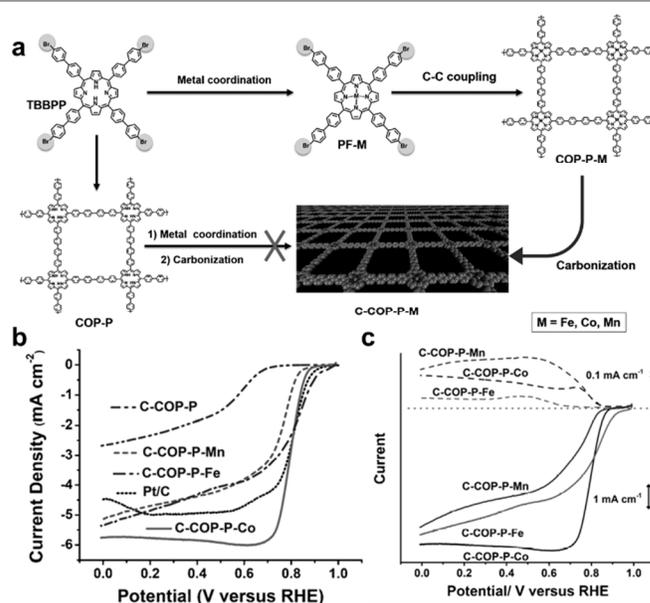
Fig. 7. a) The incorporation of non-precious metals (Fe, Co, or Mn) into C-COP in this work. b) LSV curves of metal-incorporated C-COP-P-M in O_2-saturated 0.1 M KOH at 1600 rpm at a sweep rate of 5 mV s^{-1}. c) Rotating ring-disk electrode (RRDE) voltammograms recorded with the metal-incorporated C-COP-P-M graphene in O_2-saturated 0.1 M KOH at 1600 rpm. (Reproduced from ref. 67 with permission. Copyright 2014, John Wiley & Sons)

The electron transfer number of C-COP-Fe and C-COP-Co was 3.81 and 3.56, respectively. The electron transfer number calculated from the rotating ring-disk electrode (RRDE) measurements (Figure 7c) confirms a nearly 4-electron oxygen reduction pathway. Furthermore, all of the three C-COP-P-M electrodes were not affected from methanol crossover, but these samples exhibits slightly decreased CO poisoning (*c.a.* 0%). This results indicated that C-COP-P-M electrode much stable from the CO poisoning than that of Pt/C (80% decreased). In addition, the resultant metal-incorporated C-COP materials were found to show efficient electrocatalytic activities toward 4e oxygen reduction in both alkaline and acid media with an excellent stability such as methanol crossover and CO poisoning effect than that of the Pt/C. Clearly, therefore, these newly-developed metal-incorporated C-COP materials seem to hold great potential as efficient ORR catalysts for fuel cells in both alkaline and acidic medium.

Conclusions, prospect and Outlook

In this review, recent developments of non-precious metal catalysts for ORR in fuel cells are discussed. For a sustainable fuel cell commercialization, developing active, durable, and non-precious metal catalysts to replace currently used expensive Pt-based catalysts is a prerequisite. Summarizing various preparation methods, ORR kinetics, and fuel cell performances of non-precious metal catalysts; focus is paid on Fe and Co based catalysts. Up to day, several advances have been made in developing cheaper and eco-friendly synthesis routes to enhancing not only the catalytic activity and durability, but also selectivity towards the ORR, to improve fuel cell performance. Graphene-supported non-precious metal electrocatalysts for ORR are also reviewed, that include non-pyrolyzed and pyrolyzed metal nitrogen-containing complexes. Graphene supported non-precious metal catalysts shows big improved stability because it led to prevent aggregation of non-precious metal and increase the catalytic activities. Among these candidates, pyrolyzed carbon supported nitrogen containing non-precious metal catalysts show better electrocatalytic activities and stability for ORR. While significant advances have been realised in basic or alkaline media, a pressing challenge however involves the development of non-precious catalysts for devices operating in acidic media. With operational stability being one of the current limiting factor, catalyst utilization and improving the ORR activity of such non-precious metal catalyst is still a short-term research and development priority. Only if the ORR activity successfully approaches the provided targets, research and development into improving the stability of these materials will move to the forefront of investigations. As the cost of non-precious catalysts pales in comparison with platinum based catalysts, significantly higher catalyst loading is also feasible ensuring catalyst layer thickness with improved ORR activity. In future, the development of high-performance non-precious metal/metal-free catalysts is imperative and is expected to provide immense economic advantages with improved electrocatalytic activities over Pt/C catalysts with good stability, tolerance to CO poisoning and fuel crossover effect.

Acknowledgements

Notes and references

^{a} School of Energy and Chemical Engineering/Low-Dimensional Carbon Materials Center, Ulsan National Institute of Science and Technology (UNIST), 100, Banyeon, Ulsan 689-798, South Korea

† Authors contributed equally.

1. M. Z. Jacobson, W. G. Colella and D. M. Golden, *Science*, 2005, **308**, 1901-1905.
2. M. G. Schultz, T. Diehl, G. P. Brasseur and W. Zittel, *Science*, 2003, **302**, 624-627.
3. M. Dresselhaus, I. Thomas, *Nature*, 2001, **414**, 332-337.
4. C. K. Dyer, *J. Power Sources*, 2002, **106**, 31-34.
5. A. Heinzel, C. Hebling, M. Müller, M. Zedda and C. Müller, *J. Power Sources*, 2002, **105**, 250-255.
6. W. Sheng, H. A. Gasteiger and Y. Shao-Horn, *J. Electrochem. Soc.*, 2010, **157**, B1529-B1536.
7. J. K. B. James, in DOE-EERE Fuel Cell Technologies Program-2009 DOE Hydrogen Program Review, (www.hydrogen.energy.gov/pdfs/review09/fc_30_james.pdf)
8. S. Guo and S. Sun, *J. Am. Chem. Soc.*, 2012, **134**, 2492-2495.
9. K. A. Kuttiyiel, K. Sasaki, Y. Choi, D. Su, P. Liu and R. R. Adzic, *Energ. Environ. Sci.*, 2012, **5**, 5297-5304.
10. A. Morozan, B. Jousselme and S. Palacin, *Energ. Environ. Sci.*, 2011, **4**, 1238-1254.
11. Y. Liang, Y. Li, H. Wang, J. Zhou, J. Wang, T. Regier and H. Dai, *Nat. Mater.*, 2011, **10**, 780-786.
12. Z.-S. Wu, S. Yang, Y. Sun, K. Parvez, X. Feng and K. Müllen, *J. Am. Chem. Soc.*, 2012, **134**, 9082-9085.
13. S. Wang, L. Zhang, Z. Xia, A. Roy, D. W. Chang, J.-B. Baek and L. Dai, *Angew. Chem. Int. Ed.*, 2012, **51**, 4209-4212.
14. L. Yang, S. Jiang, Y. Zhao, L. Zhu, S. Chen, X. Wang, Q. Wu, J. Ma, Y. Ma and Z. Hu, *Angew. Chem.*, 2011, **123**, 7270-7273.
15. I.-Y. Jeon, H.-J. Choi, M. Choi, J.-M. Seo, S.-M. Jung, M.-J. Kim, S. Zhang, L. Zhang, Z. Xia, L. Dai, N. Park and J.-B. Baek, *Sci. Rep.*, 2013, **3**, 2260.
16. S. Chen, J. Bi, Y. Zhao, L. Yang, C. Zhang, Y. Ma, Q. Wu, X. Wang and Z. Hu, *Adv. Mater.*, 2012, **24**, 5593-5597.
17. C. Zhang, N. Mahmood, H. Yin, F. Liu and Y. Hou, *Adv. Mater.*, 2013, **25**, 4932-4937.
18. I.-Y. Jeon, S. Zhang, L. Zhang, H.-J. Choi, J.-M. Seo, Z. Xia, L. Dai and J.-B. Baek, *Adv. Mater.*, 2013, **25**, 6138-6145.

19. M. Liu, R. Zhang and W. Chen, *Chem. Rev.*, 2014, **114**, 5117-5160.
20. X. K. Kong, C. L. Chen and Q. W. Chen, *Chem. Soc. Rev.*, 2014, **43**, 2841-2857.
21. Q. Liu and J. Zhang, *Langmuir*, 2013, **29**, 3821-3828.
22. M. R. Gao, Y. F. Xu, J. Jiang and S. H. Yu, *Chem. Soc. Rev.*, 2013, **42**, 2986-3017.
23. R. Jasinski, *Nature*, 1964, **201**, 1212-1213.
24. K. S. Novoselov, A. K. Geim, S. V. Morozov, D. Jiang, M. I. Katsnelson, I. V. Grigorieva, S. V. Dubonos and A. A. Firsov, *Nature*, 2005, **438**, 197-200.
25. A. Peigney, C. Laurent, E. Flahaut, R. R. Bacsa and A. Rousset, *Carbon*, 2001, **39**, 507-514.
26. C. Mattevi, G. Eda, S. Agnoli, S. Miller, K. A. Mkhoyan, O. Celik, D. Mastrogiovanni, G. Granozzi, E. Garfunkel and M. Chhowalla, *Adv. Funct. Mater.*, 2009, **19**, 2577-2583.
27. C. Lee, X. Wei, J. W. Kysar and J. Hone, *Science*, 2008, **321**, 385-388.
28. L. Cui, T. Pu, Y. Liu and X. He, *Electrochim. Acta*, 2013, **88**, 559-564.
29. W. Song, C. He, W. Zhang, Y. Gao, Y. Yang, Y. Wu, Z. Chen, X. Li and Y. Dong, *Carbon*, 2014, **77**, 1020-1030.
30. A. Chunder, T. Pal, S. I. Khondaker and L. Zhai, *J. Phys. Chem. C*, 2010, **114**, 15129-15135.
31. N. Karousis, J. Ortiz, K. Ohkubo, T. Hasobe, S. Fukuzumi, Á. Sastre-Santos and N. Tagmatarchis, *J. Phys. Chem. C*, 2012, **116**, 20564-20573.
32. T. Umeyama, J. Mihara, N. Tezuka, Y. Matano, K. Stranius, V. Chukharev, N. V. Tkachenko, H. Lemmetyinen, K. Noda, K. Matsushige, T. Shishido, Z. Liu, K. Hirose-Takai, K. Suenaga and H. Imahori, *Chem. Eur. J.*, 2012, **18**, 4250-4257.
33. D. Kiessling, R. D. Costa, G. Katsukis, J. Malig, F. Lodermeyer, S. Feihl, A. Roth, L. Wibmer, M. Kehrer, M. Volland, P. Wagner, G. G. Wallace, D. L. Officer and D. M. Guldi, *Chem. Sci.*, 2013, **4**, 3085-3098.
34. J. N. Lekitima, K. I. Ozoemena, C. J. Jafta, N. Kobayashi, Y. Song, D. Tong, S. Chen and M. Oyama, *J. Mater. Chem. A*, 2013, **1**, 2821-2826.
35. Y. Li, W. Zhou, H. Wang, L. Xie, Y. Liang, F. Wei, J.-C. Idrobo, S. J. Pennycook and H. Dai, *Nat. Nanotechnol.*, 2012, **7**, 394-400.
36. D. Huang, J. Lu, S. Li, Y. Luo, C. Zhao, B. Hu, M. Wang and Y. Shen, *Langmuir*, 2014, **30**, 6990-6998.
37. R. Chen, H. Li, D. Chu and G. Wang, *J. Phys. Chem. C*, 2009, **113**, 20689-20697.
38. L. Cui, G. Lv, Z. Dou and X. He, *Electrochim. Acta*, 2013, **106**, 272-278.
39. X. Gao, J. Wang, Z. Ma and J. Ye, *Electrochim. Acta*, 2014, **130**, 543-550.
40. N. Cheng, R. Kutz, C. Kemna and A. Wieckowski, *J. Electroanal. Chem.*, 2013, **705**, 8-12.
41. J. Geng and H.-T. Jung, *J. Phys. Chem. C*, 2010, **114**, 8227-8234.
42. Q. He, Q. Li, S. Khene, X. Ren, F. E. López-Suárez, D. Lozano-Castelló, A. Bueno-López and G. Wu, *J. Phys. Chem. C*, 2013, **117**, 8697-8707.
43. J. H. Zagal, F. Bedioui and J.-P. Dodelet, *N₄-macrocyclic metal complexes*, Springer, 2007.
44. M. Jahan, Q. Bao and K. P. Loh, *J. Am. Chem. Soc.*, 2012, **134**, 6707-6713.
45. H. Tang, H. Yin, J. Wang, N. Yang, D. Wang and Z. Tang, *Angew. Chem.*, 2013, **125**, 5695-5699.
46. L. Li, R. Ma, Y. Ebina, K. Fukuda, K. Takada and T. Sasaki, *J. Am. Chem. Soc.*, 2007, **129**, 8000-8007.
47. J.-M. You, H. S. Han, H. K. Lee, S. Cho and S. Jeon, *Int. J. Hydrogen. Energ.*, 2014, **39**, 4803-4811.
48. L. Jiang, M. Li, L. Lin, Y. Li, X. He and L. Cui, *RSC Adv.*, 2014, **4**, 26653-26661.
49. H. Yin, C. Zhang, F. Liu and Y. Hou, *Adv. Funct. Mater.*, 2014, **24**, 2930-2937.
50. Y. Zhao, C. Hu, Y. Hu, H. Cheng, G. Shi and L. Qu, *Angew. Chem. Int. Ed.*, 2012, **51**, 11371-11375.
51. J. Chlistunoff, *J. Phys. Chem. C*, 2011, **115**, 6496-6507.
52. C. Zhang, R. Hao, H. Yin, F. Liu and Y. Hou, *Nanoscale*, 2012, **4**, 7326-7329.
53. X. Zhou, C. Liu, J. Liao, T. Lu and W. Xing, *J. Power Sources*, 2008, **179**, 481-488.
54. Y. Jiang, Y. Lu, X. Lv, D. Han, Q. Zhang, L. Niu and W. Chen, *ACS Catal.*, 2013, **3**, 1263-1271.
55. G. Lv, L. Cui, Y. Wu, Y. Liu, T. Pu, X. He, *Phys. Chem. Chem. Phys.* 2013, **15**, 13093-13100.
56. H. Dai, *Acc. Chem. Res.*, 2002, **35**, 1035-1044.
57. A. A. Balandin, S. Ghosh, W. Bao, I. Calizo, D. Teweldebrhan, F. Miao and C. N. Lau, *Nano Lett.*, 2008, **8**, 902-907.
58. I. Hijazi, T. Bourgeteau, R. Cornut, A. Morozan, A. Filoramo, J. Leroy, V. Derycke, B. Jousselme and S. Campidelli, *J. Am. Chem. Soc.*, 2014, **136**, 6348-6354.
59. G. Dong, M. Huang and L. Guan, *Phys. Chem. Chem. Phys.*, 2012, **14**, 2557-2559.
60. H. Li, Z. Xu, K. Li, X. Hou, G. Cao, Q. Zhang and Z. Cao, *J. Mater. Chem.*, 2011, **21**, 1181-1186.
61. M.-Q. Wang, W.-H. Yang, H.-H. Wang, C. Chen, Z.-Y. Zhou and S.-G. Sun, *ACS Catal.*, 2014, DOI: 10.1021/cs500673k, 3928-3936.
62. S. N. Goubert-Renaudin and X. Zhu, *J. Electrochem. Soc.*, 2012, **159**, B426-B429.
63. S. N. Goubert-Renaudin, X. Zhu and A. Wieckowski, *Electrochem. Commun.*, 2010, **12**, 1457-1461.
64. Y. Ji, Z. Li, S. Wang, G. Xu, D. Li and X. Yu, *J. Electrochem. Soc.*, 2011, **158**, B139-B142.
65. H.-C. Kong, X. Yuan, X.-Y. Xia and Z.-F. Ma, *Int. J. Hydrogen. Energ.*, 2012, **37**, 13082-13087.
66. D.-W. Kim, O. L. Li and N. Saito, *Phys. Chem. Chem. Phys.*, 2014, **16**, 14905-14911.
67. Z. Xiang, Y. Xue, D. Cao, L. Huang, J.-F. Chen and L. Dai, *Angew. Chem. Int. Ed.*, 2014, **53**, 2433-2437.

TOC